

000 VIDEO-IN-THE-LOOP: SPAN-GROUNDED LONG 001 002 003 004 005 006 007 008 009 010 011 012 013 014 015 016 017 018 019 020 021 022 023 024 025 026 027 028 029 030 031 032 033 034 035 036 037 038 039 040 041 042 043 044 045 046 047 048 049 050 051 052 053 VIDEO QA WITH INTERLEAVED REASONING

Anonymous authors

Paper under double-blind review

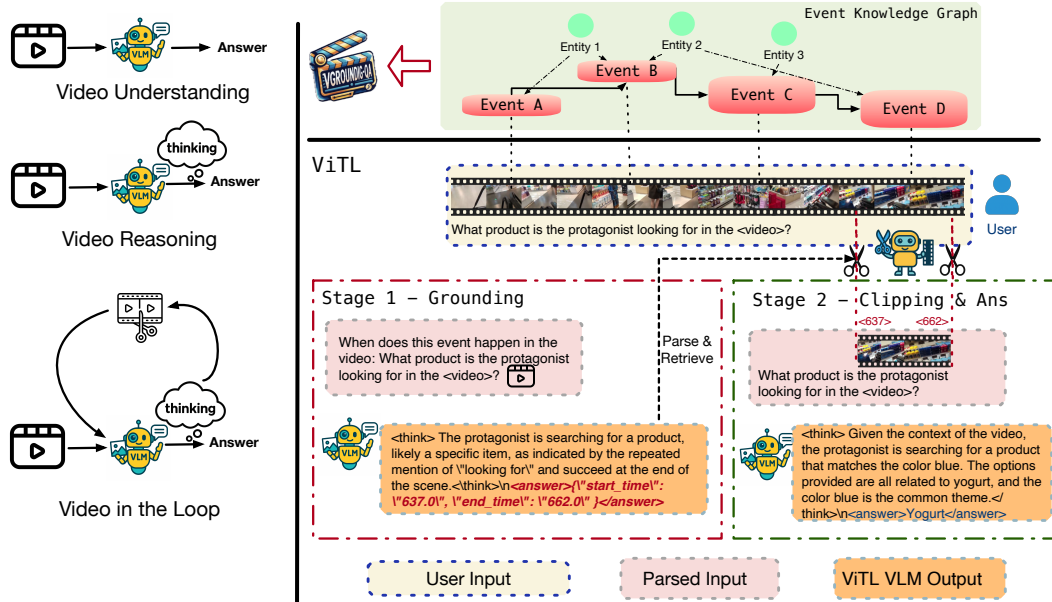


Figure 1: Overview of *ViTL* (Video-in-the-Loop) and *VGrounding-QA*. **ViTL** (right-down): Given a long video V and a question q , **Stage 1 (Ground)** takes a *grounding query distilled from q* (“locate the moments needed to answer q ”) and predicts one or multiple relevant temporal spans $S = \{[t_s^{(i)}, t_e^{(i)}]\}$. Supervision comes from event-graph *gold spans*. **Stage 2 (Answer)** re-encodes only frames within S at higher fidelity (e.g., higher frame rate/resolution) and answers the original MCQA. Training follows an R1-style loop that jointly optimizes grounding (IoU-based) and QA (cross-entropy or reward) objectives, encouraging spans that improve answering. ***VGrounding-QA*** (right-top): The spanning aware training set is achieved from Event Knowledge Graph.

ABSTRACT

We present *Video-in-the-Loop* (ViTL), a two-stage long-video QA framework that preserves a fixed token budget by first *localizing* question-relevant interval(s) with a low-fps skim and then *answering* via span-aware reallocation of visual tokens at higher effective frame rate, emitting an interleaved output with both spans and the final option for direct attribution. We also introduce *VGrounding-QA*, which converts description based event graphs into *span-grounded* multiple-choice QA by pairing each question with *ground-truth* time span(s) and related reasoning. ViTL is trained end-to-end with an interleaved group-relative objective that couples temporal IoU for localization with answer correctness, allowing credit to flow from answers back to spans without increasing compute. Under fixed token budgets, ViTL attains up to 8.6% with 50% less frame input on long-video QA and temporal grounding (e.g., Charades-STA, ActivityNet-Captions) and ablations show that span-aware token reallocation consistently surpasses uniform sampling. Together, *VGrounding-QA* and ViTL provide an interpretable, compute-efficient recipe for scalable long-video QA.

054 1 INTRODUCTION
055
056

057 Multimodal large language models (MLLMs) have advanced rapidly (Hurst et al., 2024; Li et al.,
058 2024a; OpenGVLab Team, 2024), showing strong performance in instruction following, open-
059 vocabulary perception, and multi-step reasoning across images and videos. Recent systems extend
060 temporal context windows, add memory modules, and leverage stronger backbones (e.g., 3B–70B+
061 vision language models), making long-form understanding an increasingly realistic goal.

062 Despite rapid progress, long-video QA remains brittle. Under fixed token and frame budgets, models
063 typically adopt uniform or heuristic sampling (Team, 2025; Lin et al., 2023), spending most capacity
064 on background and overlooking the brief moments that carry the answer. Public training sets (Gao
065 et al., 2017; Fu et al.; Wu et al.) rarely bind each question to *ground-truth* temporal spans, so systems
066 learn to produce answers without reliably learning *where* to look—hindering attribution and limiting
067 evaluation beyond accuracy. Moreover, localization and answering are often optimized in isolation;
068 even when span prediction improves (e.g., higher tIoU), those gains do not consistently translate
069 into better QA because the learning signal does not reward spans that actually improve answers.

070 Recent efforts extend context windows and adopt adaptive or key-frame selection to reduce back-
071 ground dilution, yet many tokens still land off-target and attribution remains limited. *Temporal*
072 *Video Grounding (TVG)* methods (Liu et al., b; Qu et al., 2024) strengthen localization, but their
073 benefits rarely carry over to QA without span-aware training signals. R1-based post-training (Feng
074 et al.; DeepSeek-AI et al.) improves step-by-step reasoning, but in the absence of span supervision
075 and reward coupling it cannot teach *where* to search. These observations motivates us to explore a
076 pipeline that reallocates visual tokens to evidence at fixed cost (zoom-in the video), a dataset that
077 jointly supervises spans and answers, and a learning objective that couples localization quality with
078 answer utility.

079 We present *Video-in-the-Loop* (ViTL), a two-stage procedure that allocates computation where it
080 matters while preserving a fixed token budget. The model first performs a low-frame-rate *skim* over
081 the entire video to localize one or more evidence intervals, then *zooms* into the predicted spans and
082 reasons at a higher effective frame rate to produce the multiple-choice answer. Both the localized
083 spans and the final option are emitted in a single, interleaved response, yielding direct attribution
084 and a uniform format for evaluation. By design, ViTL turns long-video QA into a skim→zoom
085 workflow that concentrates tokens on evidence rather than background (see Fig. 1).

086 We train ViTL end-to-end on the interleaved output using a group-relative policy objective (GRPO)
087 that couples a temporal-IoU signal for span quality with an answer-correctness signal for utility.
088 This composite reward assigns credit from the answering step back to the localization step, so spans
089 are optimized not merely to match annotations but to improve downstream answers under the same
090 compute. A brief supervised warm-up stabilizes decoding, after which interleaved GRPO refines
091 both stages jointly and encourages the model to produce well-formed spans and faithful answers in
092 one pass.

093 However, in long-video understanding tasks, accurately identifying the time segments relevant to a
094 given question is highly challenging, since many questions are complex, may span multiple tem-
095 poral segments, and often involve intricate temporal and object relationships. To address this, we
096 innovatively apply *event knowledge graph* techniques: powerful MLLMs such as GPT-4o are first
097 employed to perform fine-grained structured analysis of the entire video, extracting objects, events,
098 and their relationships to construct an event knowledge graph. From this graph, we then select val-
099 uable nodes and edges to formulate QA questions. In this way, we can design multi-hop reasoning
100 questions that span multiple temporal segments, which enables us to train models to simultaneously
101 improve both temporal localization of question-relevant segments and the ability to handle complex
102 long-video understanding problems. (see Fig. 2)

103 Our contributions can be summarized as follows:

104 (1) We introduce a *Video-in-the-Loop* procedure that reallocates tokens to predicted evidence under
105 a fixed budget, producing interpretable span grounding and answers.

106 (2) We develop a span-grounded training set construction approach and a training set called
107 *VGrounding-QA* that ties each QA item to *ground-truth* temporal spans, supplying the missing su-
pervision for span-aware QA.

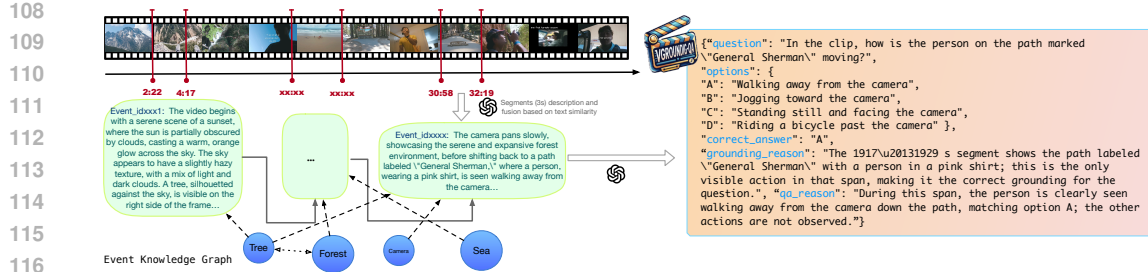


Figure 2: **Training-set construction from event graphs via semantic chunking.** A long video is first buffered into short uniform chunks (e.g., 3s) and produces per-chunk descriptions. Neighboring chunks with high textual similarity are merged into *semantic segments*; their absolute start/end times become the **ground-truth** span(s) (example: 30:58 → 32:19). Each segment is summarized into an event description and converted into a *span-grounded* MCQA instance whose question is answerable using only this span; distractors are mined from other events in the same video.

(3) We perform end-to-end training that links temporal IoU and answer reward, providing direct credit assignment from answers back to spans.

(4) We evaluate on **long-video QA** and **temporal grounding**, and conduct ablations to demonstrate the effectiveness of the proposed paradigm.

2 RELATED WORK

2.1 MLLMs FOR LONG-VIDEO UNDERSTANDING

Recent multimodal LLMs extend language reasoning to video by enlarging temporal context, compressing visual tokens, and adding spatio-temporal adapters. LLaMA-VID reduces per-frame tokens to support hour-scale inputs (Li et al., 2024b); VideоЛLaMA2 introduces specialized temporal connectors and an audio branch for richer dynamics (Cheng et al., 2024); and LongVA pushes sequence length into the hundred-thousand-token regime for untrimmed videos (Zhang et al., 2024b). Concurrently, video-tuned backbones (e.g., Qwen2.5-VL; Video-LLaVA) demonstrate strong zero-/few-shot results on captioning and QA (Team, 2025; Lin et al., 2023). Reasoning-centric post-training has also been explored: rule-based RL improves step-by-step solutions in text (Guo et al., 2025) and has been adapted to video settings (Feng et al., 2025). On the localization front, *temporal video grounding* integrates language with segment prediction and is commonly evaluated on Charades-STA and ActivityNet-Captions (Gao et al., 2017; Krishna et al., 2017); recent LLM-based approaches (Ren et al., 2023; Huang et al., 2024; Qian et al., 2024; Zhao et al., 2024) report stronger tIoU/Recall. While effective at broad coverage and zero-shot generalization, many systems still operate over globally sampled frames and rely on training protocols that optimize grounding and answering separately, which can leave attribution and span-to-answer transfer underexploited.

2.2 MULTI-STAGE AND ADAPTIVE VIDEO PROCESSING

A complementary line reduces redundancy by selecting key frames or segments before reasoning. Baselines rely on uniform or heuristic sampling, while recent methods use semantics-aware selection with VLMs such as CLIP (Radford et al., 2021)—e.g., BOLT (Liu et al., a) and AKS (Tang et al., 2025) retrieve frames most aligned with a text query and then feed them to a larger model. This improves efficiency and can outperform uniform/ k picks on long videos.

While effective, CLIP-based selection inherits a query-embedding mismatch: interrogative questions are not the distribution CLIP was trained on, so retrieved frames maximize caption-style alignment rather than evidential sufficiency for the posed question. Moreover, top- k retrieval over individual frames tends to break temporal continuity—dropping onsets/offsets and interstitial motion—thereby introducing “negative” frames and missing multi-span evidence crucial for actions and causality. Because the selector is optimized with proxy salience objectives and sits upstream of answering, utility cannot flow back to refine selection, which makes performance sensitive to thresholds and limits temporal attribution.

162 3 *VGrounding-QA: TRAINING SET CREATION FROM EVENT GRAPHS*
163164
165 **Overview.** We construct a span-grounded training set that couples *verifiable temporal supervision*
166 with *answer supervision* as exemplified in Figure 2. Our pipeline proceeds in three stages: (i) se-
167 lecting source annotations with broad coverage, (ii) converting each annotated event into a single
168 MCQA instance that is answerable from its **ground-truth** temporal span(s), and (iii) performing lay-
169 ered quality review to ensure temporal locality and item difficulty. Table 2 shows a breif comparison
170 with existing long video understanding datasets.
171172 **Event Knowledge Graph construction.** We adopt event graphs built by a *semantic chunking*
173 pipeline from prior work (Yan et al., 2025). Instead of uniform, fixed-window segmentation alone,
174 a long video is first buffered into short, uniform chunks (e.g., ~ 3 s). A lightweight VLM (e.g., a
175 7B variant) then produces a brief description for each chunk. Neighboring chunks are compared via
176 a text-similarity signal (BERTScore over the per-chunk descriptions); adjacent chunks with high
177 similarity are *merged* into a single, temporally contiguous *semantic chunk*, while boundaries are
178 enforced where similarity drops below a threshold. This yields event-level segments that better
179 match the variable temporal granularity of real videos and remain efficient to construct under tight
180 compute. Each semantic chunk is further summarized to obtain a concise event description, and its
181 absolute start/end times define the event’s **ground-truth** span(s). Edges between events are derived
182 from interval relations on these spans (e.g., *Before*, *Overlaps*). Entities are retrieved and linked from
183 each events with semantic de-duplication through embedding based clustering. Entities within the
184 same cluster are then linked.
185186 **Conversion to span-grounded QA.** For every event node, we first inherit and normalize its span
187 set: timestamps are converted to seconds, spans are sorted and minimally merged when slightly
188 overlapping, invalid ranges are removed, and disjoint occurrences are retained as multi-span. We
189 then distill a short, entity/attribute-aware *grounding query* from the node description using GPT-
190 o3 API (Hurst et al., 2024); deictic phrasing (“this clip/moment”) is avoided so the text remains
191 globally localizable on the timeline. Finally, we synthesize exactly one multiple-choice question
192 (four options) conditioned on the event and its span(s). The question must be answerable using only
193 the annotated evidence (the union when multi-span), and the three distractor options are drawn from
194 other events in the *same video* to provide realistic, in-domain confounds. Brief rationales for span
195 sufficiency (Stage 1) and option correctness (Stage 2) may be retained for supervised learning input.
196197 **Quality review.** We apply a compact but strict review stack. First, schema validity ensures a single
198 correct option and parsable fields. Second, temporal-locality checks reject items whose resolution
199 requires frames outside the annotated span set or relies on purely holistic summaries; for multi-
200 span events, items must genuinely require the annotated union when the narrative spans multiple
201 segments. Third, language screening removes deictics and vague stems, keeping questions specific
202 yet video-dependent. Fourth, a text-only screening step is applied to filter items that can be reliably
203 answered without the video; such items are revised or discarded. Finally, near-duplicates within a
204 video are removed, and option labels are balanced to avoid positional bias.
205206 **Record schema.** Each instance minimally contains the fields in Table 1. Stage 1 uses the *ground-*
207 *ing query* and *ground-truth spans* for temporal localization; Stage 2 uses the clipped segment(s)
208 together with *question*, *options*, and *correct answer* for answer supervision.
209210 **Splits and reporting.** Data are split by *video* to prevent leakage from shared footage. We keep
211 domain and duration distributions comparable across splits and preserve the prevalence of multi-
212 span items. Aggregate counts, span-length statistics (mean/median and percentiles), the propor-
213 tion of multi-span instances, per-video instance counts, and option-label balance are reported in the
214 Appendix. The resulting training set pairs **verifiable spans** for temporal grounding with **multiple-
215 choice supervision** for answering. Same-video distractors make localization consequential under a
fixed token budget, aligning the data directly with the two-stage protocol in Sec. 4.
216

216 Table 1: Minimal schema for each training instance. GT = ground truth.
217

218 Field	219 Role
220 video_id, event_id	Link to the source video and event node
221 time_spans (GT)	Supervision for Stage 1 grounding (tIoU/Recall); single or multi-span
222 event_description	Human-readable summary of the event node
223 grounding_query	Span-seeking reformulation for Stage 1 localization
224 question	Prompt for Stage 2 reasoning on the clipped segment(s)
225 options (A-D), correct_answer	Supervision for Stage 2 answer selection
226 stage1_reason, stage2_reason	Optional signals (span sufficiency; option justification)

227 Table 2: Comparison of long-video resources. “MCQA” = multiple-choice QA; “Multi-span” =
228 multiple disjoint spans; “Reason” = per-sample reasoning fields.
229

230 Dataset	231 GT spans	232 MCQA	233 Multi-span	234 Event-graph	235 Reason
236 Charades-STA	✓				
237 ActivityNet-Captions (VTG splits)	✓		(rare)		
238 LongVideoBench / LVBench / MLVU		✓			
239 VGrounding-QA (ours)	✓	✓	✓	✓	✓

240

4 ViTL: INTERLEAVED TWO-STAGE GRPO WITH GROUNDED SPANS

241

4.1 TWO-STAGE VIDEO-IN-THE-LOOP WITH FRAME-LEVEL TIMESTAMP INJECTION

242 **Formulation.** Given a long video V of duration $|V|$ and a question Q , the model predicts (i) a
243 set of temporal segments $T = \{[t_s^{(m)}, t_e^{(m)}]\}_{m=1}^M$ that contain the necessary evidence, and (ii) a
244 multiple-choice answer $A \in \{A, B, C, D\}$. Training/evaluation uses *ground-truth* spans \mathcal{T}^* inherited
245 from the event graph (Sec. 3); we allow $M \geq 1$ (multi-span).

246 **Stage 1: Global temporal localization.** We sample a *global* sequence of n_g frames uniformly
247 over $[0, |V|]$ to obtain $V_g = \{(x_f, t_f)\}_{f=1}^{n_g}$, where t_f is the absolute time (in seconds) and x_f is the
248 image token. Conditioned on Q and a short grounding query, the model outputs a structured set of
249 segments

$$T = \{[t_s^{(m)}, t_e^{(m)}]\}_{m=1}^M, \quad 0 \leq t_s^{(m)} < t_e^{(m)} \leq |V|,$$

250 together with a brief rationale. We permit M to vary up to M_{\max} ; disjoint segments are encouraged
251 when the evidence is non-contiguous.
252

253 **Stage 2: Span-conditioned answering.** Let $U(T)$ denote the (ordered) union of predicted segments.
254 We clip V to $U(T)$ and sample a *local* sequence of n_ℓ frames at higher effective fps, yielding
255 $V_\ell = \{(x_f, t_f)\}_{f=1}^{n_\ell}$ with the *same absolute timestamps* t_f (no re-zeroing). Conditioned on
256 (Q, T, V_ℓ) the model outputs the final option A and a short justification. This reallocates visual
257 tokens from background to evidence while keeping the total budget $n_g + n_\ell$ fixed.
258

259 **Frame-level timestamp injection (textual).** To stabilize temporal reference and enable auditable
260 spans, each frame is serialized as an image token followed by a human-readable absolute time:

$$\langle \text{image} \rangle @ t_1 \text{s}, \langle \text{image} \rangle @ t_2 \text{s}, \dots, \langle \text{image} \rangle @ t_F \text{s},$$

263 We require Stage 1 to emit spans as $\langle \text{span} \rangle [\hat{t}_s, \hat{t}_e] \langle / \text{span} \rangle$ and Stage 2 to answer *using only*
264 frames whose timestamps lie within $U(T)$. Ablations in Sec. 5.4 show that this textual timestamping
265 improves tIoU/Recall and reduces off-by-segment errors under the same token budget.
266

267 **Budgets and sampling policy.** Unless otherwise specified, we use n_g uniformly spaced frames
268 for Stage 1 over $[0, |V|]$ and n_ℓ frames for Stage 2 drawn from $U(T)$ (with per-span caps to prevent
269 degenerate allocation). Segments in T are sorted and minimally merged prior to clipping; multi-span
inputs are concatenated in temporal order.

270 **Validity constraints.** Outputs are lightly constrained at the prompt level: Stage 1 must place seconds inside `...` with numeric values (two decimals), and Stage 2 must emit exactly one option inside `<answer>...</answer>`. During training, malformed or out-of-range spans are rejected by format checks; at evaluation they are treated as invalid.

275 4.2 LEARNING WITH INTERLEAVED GROUP-RELATIVE POLICY OPTIMIZATION

277 **GRPO on interleaved sequences.** We optimize π_θ with Group-Relative Policy Optimization (GRPO) on interleaved outputs. For each (Q, V) we sample k responses $\{S_i\}_{i=1}^k$, each $S_i = [T_i; A_i]$, and compute group-relative advantages $A_i = R_i - \frac{1}{k} \sum_{j=1}^k R_j$. The objective maximizes the likelihood of higher-reward sequences:

$$282 \quad \mathcal{L}_{\text{GRPO}} = -\mathbb{E}_{(Q, V)} \sum_{i=1}^k A_i \log \pi_\theta(S_i \mid V_{\text{unified}}, Q). \quad (1)$$

284 Coupling both stages within S provides direct credit assignment from answer utility back to localization.

287 **Composite reward with span utility.** Each response $S = [T; A]$ is scored by

$$289 \quad R(S) = (1 - \gamma) R_{\text{loc}}(T) + \gamma R_{\text{ans}}(A), \quad \gamma \in [0, 1]. \quad (2)$$

290 Localization uses a multi-span temporal IoU against ground truth plus a small format component:

$$292 \quad R_{\text{loc}}(T) = (1 - \alpha) \text{tIoU}(T, \mathcal{T}^*) + \alpha \text{Fmt}_{\text{time}}(T),$$

293 where tIoU is the ratio of total intersection to total union length over time; Fmt_{time} rewards in-range, 294 ordered, well-formed timestamps. The answer term rewards exact match and stable formatting:

$$295 \quad R_{\text{ans}}(A) = (1 - \beta) \mathbb{1}[A = A^*] + \beta \text{Fmt}_{\text{ans}}(A).$$

296 Small α, β stabilize learning without outweighing task reward. Invalid or unparsable spans receive 297 near-zero Fmt_{time} .

299 **Initialization, schedule, and controls.** We initialize from a base VLM (e.g., Qwen2.5-VL-
300 3B/7B). A short supervised warm-up on MCQA *clipped to ground-truth spans* stabilizes decoding.
301 We then run interleaved GRPO with group size k (e.g., $k=3$), per-batch reward normalization, and
302 KL control to the base policy. A light curriculum gradually increases γ from localization-heavy to
303 answer-balanced over early epochs. Full hyperparameters appear in Sec. 5.1.

305 5 EXPERIMENTS

307 5.1 SETUP

309 **Long-video QA benchmarks.** We evaluate on three public QA suites with multi-choice format and
310 long, open-domain videos: **LongVideoBench** (Val split), **LBench** (Val), and **MLVU** (Dev), where
311 we report accuracy (%). For MLVU we additionally report the **Needle QA** subset (temporal retrieval
312 stress test) and the macro average **M-Avg** across tasks.

313 **Temporal Video Grounding (TVG) benchmarks.** We use **Charades-STA** (indoor activities;
314 trimmed queries on untrimmed videos) and **ActivityNet-Captions** (open-domain activities). Following
315 standard practice, we report **Recall@IoU={0.3, 0.5, 0.7}** and **mIoU** (%).

317 **Role of our event-graph dataset.** Our event-graph grounded dataset (Sec. 3) provides *training*
318 and *diagnostic* supervision: each question is paired with *gold* time span(s) derived from an event
319 graph, enabling learnable temporal grounding and auditable evaluation. Unless otherwise specified,
320 this dataset is not used as a held-out test set; all reported results use the official public splits of the
321 benchmarks above.

322 **Evaluation protocol and fairness.** To ensure comparability, all systems run under matched com-
323 pute budgets. We report (when applicable) *frames* per question and keep the total token/FLOPs

324 budget fixed across baselines. Unless stated, we do not use external subtitles/ASR. Inference for
 325 *ViTL* is two-stage: a low-fps global sweep for *localization* (Stage 1), followed by span-aware high-
 326 fidelity *answering* (Stage 2). Results are reported on $4 \times$ A100 80G; hyper-parameters are provided
 327 in the Appendix for reproducibility.

329 **Backbones.** We instantiate *ViTL* with **Qwen2.5-VL 3B** and **Qwen2.5-VL 7B**. Unless otherwise
 330 noted, Stage 1 and Stage 2 share the same backbone. In a compute-efficient setting, we also study a
 331 light *selector* (3B) with a stronger *answerer* (7B) in Sec. A.

333 **Training protocol.** We adopt a simple three-step schedule that closes the loop between localization
 334 and answering while keeping budgets explicit. **(T1) Supervised warm-up.** *Grounding SFT*: train
 335 Stage 1 with IoU-based span supervision on our event-graph dataset (gold span(s) per question);
 336 we minimize a boundary/IoU loss. *QA SFT*: train Stage 2 on the paired MCQA (cross-entropy over
 337 options), using only frames within the *gold* spans. For TVG benchmarks, we do not fine-tune on their
 338 train splits unless explicitly marked as FT. **(T2) Two-stage coupling (teacher forcing).** We connect
 339 the stages by feeding Stage 1 predictions into Stage 2. To stabilize learning, we sample a fixed ratio
 340 of teacher-forced spans (gold) and model spans (predicted) during training, and restrict Stage 2’s
 341 visual budget to the union of selected span(s). **(T3) R1-style post-training.** We optimize a weighted
 342 reward that encourages spans which *improve answering*: *TVG reward* = IoU with gold span(s)
 343 (shape with thresholds), *QA reward* = 1 for correct option and 0 otherwise (plus mild format/length
 344 penalties). We apply PPO with a KL penalty to the SFT reference; gradients update both stages.
 345 The overall objective is a weighted sum of TVG and QA terms; ablations over these weights are in
 346 Sec. 5.4.

347 **Inputs and budgets.** Stage 1 consumes a fixed number of frames (e.g., 64 frames) and takes the
 348 global view of the full video and a *grounding query* distilled from the question (“locate the moments
 349 needed to answer q ”). Stage 2 re-encodes only the predicted span(s) at higher fidelity (e.g., 4–8
 350 fps and/or higher resolution), up to K spans (default $K=5$), keeping the *total* token/frame budget
 351 matched to baselines. Unless noted, Stage 2 answers the original MCQA (no extra hints) on the
 352 clipped segment(s).

353 5.2 LONG-VIDEO QA PERFORMANCE

355 We evaluate the full *ViTL* pipeline on **LongVideoBench** (Val), **LBench** (Val), and **MLVU** (Dev).
 356 Unless noted, comparisons follow the no-subtitles, matched-preprocessing setting (global low-fps
 357 sweep; fixed resolution) for fairness. Our improvements stem from two ingredients: (i) an *event-
 358 graph* dataset that pairs reasoning-centric questions with **ground-truth** time spans (Sec. 3), enabling
 359 learnable and auditable temporal grounding; and (ii) a *two-stage, R1-style* training protocol (Sec. 4)
 360 that couples IoU-based grounding signals with QA objectives, encouraging spans that *actually* im-
 361 prove answering under fixed token/frame budgets.

362 **Discussion.** The largest gains appear on **LBench**, where relevant moments are sparse and uni-
 363 form sampling wastes budget. By learning spans from event-graph supervision and coupling
 364 them to answering with a two-stage R1-style objective, *ViTL* reallocates visual tokens toward evi-
 365 dence—achieving higher accuracy at comparable (or lower) frame budgets. An oracle-span analysis
 366 in Sec. 5.4 further quantifies the remaining headroom from localization fidelity, supporting both the
 367 dataset design and the training protocol.

369 5.3 TEMPORAL GROUNDING PERFORMANCE

371 We then assess *ViTL*’s ability to *localize* question-relevant moments. All results are zero-shot unless
 372 noted. The gains are primarily driven by two factors: (i) our *event-graph* dataset that pairs reasoning-
 373 centric questions with *groundtruth* time spans (Sec. 3), providing auditable supervision for temporal
 374 grounding; and (ii) our *two-stage, R1-style* training that jointly optimizes an IoU-based grounding
 375 signal and a QA objective, encouraging spans that improve answering (Sec. 4.2).

376 **Charades-STA (Gao et al., 2017).** This benchmark focuses on indoor activities with natural lan-
 377 guage queries. As shown in Table 4, **ViTL (Ours 7B)** surpasses specialized VTG systems across

378 Table 3: **Long-video QA benchmarks**. Accuracy (%) on **LongVideoBench** (Val), **LVBench** (Val),
 379 and **MLVU** (M-Avg). “Frames” is the per-question frame budget when available. \dagger official num-
 380 bers; \ddagger our re-test under the matched preprocessing (global low-fps sweep; uniform sampling; 448
 381 resolution). “—” indicates not reported under the same setting.

Models	Size	Frames	LongVideoBench	LVBench	MLVU M-Avg
<i>Closed Video MLLMs</i>					
GLM-4V-Plus \dagger	—	256	70.8	58.7	—
GPT-4o \dagger	—	384	66.7	27.0	64.6
Gemini-1.5-Pro \dagger	—	0.5 fps	64.0	33.1	—
<i>Small Video MLLMs</i>					
VITA-1.5	7B	16	56.1	—	—
LLaVA-Video	7B	64	58.2	—	—
LongVA	7B	128	52.1	39.4	52.0
NVILA	8B	256	57.7	—	—
ByteVideoLLM	14B	256	—	—	—
VideoLLaMA3	17B	180	59.8	45.3	—
InternVL3	8B	16–64	62.5	—	—
Qwen2.5-VL \dagger	7B	256	56.0 (224 res)	45.3	54.5
Qwen2.5-VL \ddagger	7B	256	61.8 (448 res)	43.7	—
ViTL (Qwen2.5-VL)	7B	128	63.3	47.4	62.3

398 Table 4: Zero-shot temporal grounding on Charades-STA (Gao et al., 2017). **Bold** marks our scores.

Method	Size	R@0.3 (%)	R@0.5 (%)	R@0.7 (%)	mIoU (%)
VTimeLLM (Huang et al., 2024)	13B	55.3	34.3	14.7	34.6
TimeChat (Ren et al., 2023)	7B	51.5	32.2	13.4	—
Momentor (Qian et al., 2024)	7B	42.6	26.6	11.6	28.5
HawkEye (Zhao et al., 2024)	7B	50.6	31.4	14.5	33.7
ChatVTG (Qu et al., 2024)	7B	52.7	33.0	15.9	34.9
VideoChat-TPO (Yan et al., 2024)	7B	58.3	40.2	18.4	38.1
E.T. Chat (Liu et al., 2024b)	4B	65.7	45.9	20.0	42.3
ViTL (Ours 7B)	7B	77.7	63.5	36.3	54.0

411 recall thresholds and mIoU. **ActivityNet-Captions (Krishna et al., 2017)**. Results on open-domain,
 412 untrimmed videos are shown in Table 5. **ViTL (Ours 7B)** maintains strong localization across
 413 R@IoU levels.

415 5.4 ABLATION STUDIES ON LONG-VIDEO QA

416 We quantify which ingredients drive gains under *matched token/frame budgets* and a fixed backbone
 417 (Qwen2.5-VL 3B/7B). We report accuracy (%) on **LongVideoBench** and **LVBench**. All single-
 418 stage variants consume $n_g + n_\ell$ frames uniformly over the full timeline; the two-stage system uses
 419 n_g (global skim) + n_ℓ (zoomed evidence).

420 **Settings.** A) **SFT** — single-stage supervised fine-tuning on our MCQA (no timestamps). B) **SFT**
 421 + **TI** — single-stage with *frame-level textual timestamp injection*. C) **SFT + Stage-2-only + TI**
 422 (**full video**) — no Stage 1; apply the Stage-2 answering prompt with timestamps to the *entire video*
 423 (no cropping); total frames $n_g + n_\ell$ sampled uniformly. D) **ViTL(full)** — two-stage with interleaved
 424 GRPO (coupled QA+TVG rewards) and timestamp injection in both stages.

425 **Findings.** *Timestamping improves global reasoning.* A→B isolates frame-level time tokens in a
 426 single-stage setup and yields consistent gains on both benchmarks, indicating reduced temporal
 427 ambiguity when evidence is dispersed. *Answer-centric training helps without localization.* B→C
 428 shows that the Stage-2 answering prompt with timestamps—applied to the full video at the same
 429 budget—further boosts accuracy, suggesting better temporal utilization despite no cropping. *Full*
 430 *ViTLL is best at fixed compute.* C→D adds learned localization and coupled QA+TVG rewards via in-

432 Table 5: Zero-shot temporal grounding on ActivityNet-Captions (Krishna et al., 2017). FT indicates
 433 fine-tuning on the downstream training split. **Bold** marks our scores.

Method	Size	FT	R@0.3 (%)	R@0.5 (%)	R@0.7 (%)	mIoU (%)
2D-TAN (Zhang et al., 2020)	–	✓	60.4	43.4	25.0	42.5
MMN (Zhang et al., 2021)	–	✓	64.5	48.2	29.4	46.6
VDI (Luo et al., 2023a)	–	✓	–	48.1	28.8	–
VideoChat (Li et al., 2023)	7B	✗	8.8	3.7	1.5	7.2
Video-LLaMA (Zhang et al., 2023)	7B	✗	6.9	2.1	0.8	6.5
Video-ChatGPT (Maaz et al., 2023)	7B	✗	26.4	13.6	6.1	18.9
Valley (Luo et al., 2023b)	7B	✗	30.6	13.7	8.1	21.9
ChatVTG (Qu et al., 2024)	7B	✗	40.7	22.5	9.4	27.2
Momentor (Qian et al., 2024)	7B	✗	42.9	23.0	12.4	29.3
E.T. Chat (Liu et al., 2024b)	4B	✗	24.1	12.8	6.1	18.9
ViTL (Ours 7B)	7B	✗	55.1	46.3	30.0	24.1

447 Table 6: **Ablations on long-video QA (fixed token budget).** Accuracy (%). Higher is better.

Config	LongVideoBench ↑	LVBench ↑
A) SFT (single, no TI)	61.3	40.2
B) SFT + Timestamp Injection (single)	62.1	44.3
C) SFT + Stage-2-only + TI (full video; no crop)	62.5	45.4
D) ViTL(full): two-stage + GRPO (QA+TVG) + TI	63.5	47.9

456 interleaved GRPO. Accuracy improves on both datasets, confirming that allocating tokens to predicted
 457 evidence (while keeping totals fixed) yields better answers than any single-stage alternative.

459 5.5 EFFECTIVENESS OF LEARNED GROUNDING

461 To validate the necessity of a learned grounding module, we compare *ViTL* against heuristic base-
 462 lines and establish performance bounds.

464 **Parametric vs. Non-Parametric Frame Selection.** We compare *ViTL* against a strong CLIP-
 465 based baseline (ViT-L/14), which computes the cosine similarity between the question and every
 466 frame, selecting the top-128 frames. As shown in Table 7, *ViTL* consistently yields higher accu-
 467 racy (e.g., 63.3% vs. 58.1% on LongVideoBench), demonstrating that query-conditioned parametric
 468 selection provides essential evidence that zero-shot semantic similarity misses.

470 **Performance Bounds: Random vs. Oracle Zooming.** To quantify the headroom for Stage 1
 471 localization, we establish lower bounds (random sampling) and upper bounds (oracle spans). Table 8
 472 shows that *ViTL* significantly outperforms random zooming and closes a large portion of the gap
 473 toward the oracle upper bound (e.g., capturing over half the headroom on LongVideoBench). This
 474 confirms gains are attributable to accurate temporal localization.

475 Table 7: Parametric (ViTL) vs. Non-parametric
 476 (CLIP) selection.

Method	Strategy	LVideoB	LVBench
CLIP Top- <i>k</i>	Non-param.	58.1	40.3
ViTL	Parametric	63.3	47.4

475 Table 8: Performance bounds analysis: Random
 476 vs. Oracle.

Config	Input	LVideoB	LVBench
Lower Bound	Random	55.2	39.5
ViTL	Pred. Spans	63.3	47.4
Upper Bound	GT Spans	70.5	51.4

484 5.6 MECHANISM ANALYSIS: ZOOMING AND MULTI-SPAN RETRIEVAL

485 We further disentangle the architectural decisions that drive *ViTL*’s performance.

486
 487 **Impact of Visual Zooming vs. Iterative Reasoning.** To verify that gains stem from accessing
 488 high-fidelity visual details rather than simply "thinking twice," we introduce a *Refine-only* baseline
 489 (Stage 2 reuses Stage 1's low-fps frames). As summarized in Table 9, Refine-only provides only
 490 marginal gains (56.2% vs. 56.0%), whereas *ViTL* with true Zoom achieves substantial improvements
 491 (63.3%). This proves that reallocating the visual token budget to high-resolution evidence is the
 492 primary driver of performance.

493 Table 9: Mechanism ablation (Zoom vs. Refine). Iterative reasoning alone (Refine-only) yields
 494 negligible gains; improvements stem from high-fidelity visual zooming.

Method	Mechanism	LVideoBench	LVBench
Single Stage	Direct answer	56.0	45.3
Refine-only	Think twice (low FPS)	56.2	45.7
<i>ViTL</i>	Think twice (Zoom)	63.3	47.4

501
 502 **Single vs. Multi-Span Retrieval.** Allowing the retrieval of multiple disjoint spans yields a **+2.3%**
 503 absolute accuracy gain on LVbench (47.4% vs. 45.1% with a single-span constraint). This indicates
 504 that relevant evidence in long-form videos is frequently scattered, validating our multi-span design.

505 5.7 QUALITATIVE ANALYSIS

506 To provide further insight into the behavior and capabilities of *ViTL*, Figure 1 illustrates representative
 507 an example of our model's two-stage reasoning process, showcasing its ability to generate
 508 coherent thought processes, accurately ground temporal segments, and provide correct answers.
 509 Additional qualitative examples, including comparisons with baselines and failure case analyzes,
 510 are provided in the appendix A.

513 6 CONCLUSION AND DISCUSSION

515 We cast long-video QA as allocating a fixed token budget to verifiable evidence and introduced
 516 *Video-in-the-Loop* (*ViTL*), a skim→zoom pipeline that first *localizes* evidence spans and then *answers*
 517 within them. *ViTL* trains an interleaved span+answer output end-to-end with a group-relative
 518 objective coupling temporal IoU and answer correctness, enabling credit to flow from answers back
 519 to localization. To supply supervision, we develop event knowledge graphs based approach to turn
 520 video into span-grounded MCQA that ties each question to *ground-truth* time span(s) with same-
 521 video distractors. Together, the data and method move tokens off background, make "where" ex-
 522 plicit, and improve QA and grounding under matched compute. Limitations include noise in up-
 523 stream graphs, the simplicity of MCQA versus open-ended reasoning, and RL variance; many real
 524 scenarios also require richer audiovisual cues. Promising directions include streaming *ViTL* (online
 525 skim→zoom), multi-hop reasoning across events/videos, space–time grounding with entity tracks,
 526 preference/rationale supervision for faithful attribution, and joint metrics scoring answer quality,
 527 span faithfulness, and compute.

528 529 REFERENCES

530 Anthropic. Claude 3.5 sonnet model card addendum, 2024. URL https://www-cdn-anthropic.com/fed9cc193a14b84131812372d8d5857f8f304c52/Model_Card_Claude_3_Addendum.pdf. Accessed: 2025-05-16.

534 Jinze Bai, Shuai Bai, Shusheng Yang, Shijie Wang, Sinan Tan, Peng Wang, Junyang Lin, Chang
 535 Zhou, and Jingren Zhou. Qwen-vl: A frontier large vision-language model with versatile abilities.
 536 *arXiv preprint arXiv:2308.12966*, 2023.

538 Guo Chen, Yicheng Liu, Yifei Huang, Yuping He, Baoqi Pei, Jilan Xu, Yali Wang, Tong Lu, and
 539 Limin Wang. Cg-bench: Clue-grounded question answering benchmark for long video under-
 standing, 2024a.

540 Lin Chen, Xilin Wei, Jinsong Li, Xiaoyi Dong, Pan Zhang, Yuhang Zang, Zehui Chen, Haodong
 541 Duan, Bin Lin, Zhenyu Tang, et al. Sharegpt4video: Improving video understanding and genera-
 542 tion with better captions. *arXiv preprint arXiv:2406.04325*, 2024b.
 543

544 Zesen Cheng, Sicong Leng, Hang Zhang, Yifei Xin, Xin Li, Guanzheng Chen, Yongxin Zhu, Wenqi
 545 Zhang, Ziyang Luo, Deli Zhao, et al. Videollama 2: Advancing spatial-temporal modeling and
 546 audio understanding in video-llms. *arXiv preprint arXiv:2406.07476*, 2024.

547 DeepSeek-AI, Daya Guo, Dejian Yang, Haowei Zhang, Junxiao Song, Ruoyu Zhang, Runxin Xu,
 548 Qihao Zhu, Shirong Ma, Peiyi Wang, Xiao Bi, Xiaokang Zhang, Xingkai Yu, Yu Wu, Z. F. Wu,
 549 Zhibin Gou, Zhihong Shao, Zhuoshu Li, Ziyi Gao, Aixin Liu, Bing Xue, Bingxuan Wang, Bochao
 550 Wu, Bei Feng, Chengda Lu, Chenggang Zhao, Chengqi Deng, Chenyu Zhang, Chong Ruan,
 551 Damai Dai, Deli Chen, Dongjie Ji, Erhang Li, Fangyun Lin, Fucong Dai, Fuli Luo, Guangbo Hao,
 552 Guanting Chen, Guowei Li, H. Zhang, Han Bao, Hanwei Xu, Haocheng Wang, Honghui Ding,
 553 Huajian Xin, Huazuo Gao, Hui Qu, Hui Li, Jianzhong Guo, Jiashi Li, Jiawei Wang, Jingchang
 554 Chen, Jingyang Yuan, Junjie Qiu, Junlong Li, J. L. Cai, Jiaqi Ni, Jian Liang, Jin Chen, Kai
 555 Dong, Kai Hu, Kaige Gao, Kang Guan, Kexin Huang, Kuai Yu, Lean Wang, Lecong Zhang,
 556 Liang Zhao, Litong Wang, Liyue Zhang, Lei Xu, Leyi Xia, Mingchuan Zhang, Minghua Zhang,
 557 Minghui Tang, Meng Li, Miaojun Wang, Mingming Li, Ning Tian, Panpan Huang, Peng Zhang,
 558 Qiancheng Wang, Qinyu Chen, Qishi Du, Ruiqi Ge, Ruisong Zhang, Ruizhe Pan, Runji Wang,
 559 R. J. Chen, R. L. Jin, Ruyi Chen, Shanghao Lu, Shangyan Zhou, Shanhua Chen, Shengfeng
 560 Ye, Shiyu Wang, Shuiping Yu, Shunfeng Zhou, Shuting Pan, S. S. Li, Shuang Zhou, Shaoqing
 561 Wu, Shengfeng Ye, Tao Yun, Tian Pei, Tianyu Sun, T. Wang, Wangding Zeng, Wanjia Zhao, Wen
 562 Liu, Wenfeng Liang, Wenjun Gao, Wenqin Yu, Wentao Zhang, W. L. Xiao, Wei An, Xiaodong
 563 Liu, Xiaohan Wang, Xiaokang Chen, Xiaotao Nie, Xin Cheng, Xin Liu, Xin Xie, Xingchao Liu,
 564 Xinyu Yang, Xinyuan Li, Xuecheng Su, Xuheng Lin, X. Q. Li, Xiangyue Jin, Xiaoqin Shen, Xi-
 565 aoshua Chen, Xiaowen Sun, Xiaoxiang Wang, Xinnan Song, Xinyi Zhou, Xianzu Wang, Xinxia
 566 Shan, Y. K. Li, Y. Q. Wang, Y. X. Wei, Yang Zhang, Yanhong Xu, Yao Li, Yao Zhao, Yaofeng
 567 Sun, Yaohui Wang, Yi Yu, Yichao Zhang, Yifan Shi, Yiliang Xiong, Ying He, Yishi Piao, Yisong
 568 Wang, Yixuan Tan, Yiyang Ma, Yiyuan Liu, Yongqiang Guo, Yuan Ou, Yuduan Wang, Yue Gong,
 569 Yuheng Zou, Yujia He, Yunfan Xiong, Yuxiang Luo, Yuxiang You, Yuxuan Liu, Yuyang Zhou,
 570 Y. X. Zhu, Yanhong Xu, Yanping Huang, Yaohui Li, Yi Zheng, Yuchen Zhu, Yunxian Ma, Ying
 571 Tang, Yukun Zha, Yuting Yan, Z. Z. Ren, Zehui Ren, Zhangli Sha, Zhe Fu, Zhean Xu, Zhenda
 572 Xie, Zhengyan Zhang, Zhewen Hao, Zhicheng Ma, Zhigang Yan, Zhiyu Wu, Zihui Gu, Zijia Zhu,
 573 Zijun Liu, Zilin Li, Ziwei Xie, Ziyang Song, Zizheng Pan, Zhen Huang, Zhipeng Xu, Zhongyu
 574 Zhang, and Zhen Zhang. DeepSeek-R1: Incentivizing Reasoning Capability in LLMs via Rein-
 575forcement Learning. URL <http://arxiv.org/abs/2501.12948>.

576 Jiajun Fei, Dian Li, Zhidong Deng, Zekun Wang, Gang Liu, and Hui Wang. Video-ccam: Enhancing
 577 video-language understanding with causal cross-attention masks for short and long videos, 2024.
 578 URL <https://arxiv.org/abs/2408.14023>.

579 Kaituo Feng, Kaixiong Gong, Bohao Li, Zonghao Guo, Yibing Wang, Tianshuo Peng, Junfei Wu,
 580 Xiaoying Zhang, Benyou Wang, and Xiangyu Yue. Video-R1: Reinforcing Video Reasoning in
 581 MLLMs. URL <http://arxiv.org/abs/2503.21776>.

582 Kaituo Feng, Kaixiong Gong, Bohao Li, Zonghao Guo, Yibing Wang, Tianshuo Peng, Benyou
 583 Wang, and Xiangyu Yue. Video-r1: Reinforcing video reasoning in mllms. *arXiv preprint*
 584 *arXiv:2503.21776*, 2025.

585 Chaoyou Fu, Yuhang Dai, Yongdong Luo, Lei Li, Shuhuai Ren, Renrui Zhang, Zihan Wang, Chenyu
 586 Zhou, Yunhang Shen, Mengdan Zhang, Peixian Chen, Yanwei Li, Shaohui Lin, Sirui Zhao, Ke Li,
 587 Tong Xu, Xiawu Zheng, Enhong Chen, Caifeng Shan, Ran He, and Xing Sun. Video-MME: The
 588 First-Ever Comprehensive Evaluation Benchmark of Multi-modal LLMs in Video Analysis. URL
 589 <http://arxiv.org/abs/2405.21075>.

590 Chaoyou Fu, Haojia Lin, Zuwei Long, Yunhang Shen, Meng Zhao, Yifan Zhang, Shaoqi Dong,
 591 Xiong Wang, Di Yin, Long Ma, Xiawu Zheng, Ran He, Rongrong Ji, Yunsheng Wu, Caifeng
 592 Shan, and Xing Sun. Vita: Towards open-source interactive omni multimodal llm, 2024. URL
 593 <https://arxiv.org/abs/2408.05211>.

594 Jiyang Gao, Chen Sun, Zhenheng Yang, and Ram Nevatia. Tall: Temporal activity localization
 595 via language query. In *2017 IEEE International Conference on Computer Vision (ICCV)*, pp.
 596 5277–5285, 2017. doi: 10.1109/ICCV.2017.563.

597

598 Daya Guo, Dejian Yang, Haowei Zhang, Junxiao Song, Ruoyu Zhang, Runxin Xu, Qihao Zhu,
 599 Shirong Ma, Peiyi Wang, Xiao Bi, et al. Deepseek-r1: Incentivizing reasoning capability in llms
 600 via reinforcement learning. *arXiv preprint arXiv:2501.12948*, 2025.

601

602 Bin Huang, Xin Wang, Hong Chen, Zihan Song, and Wenwu Zhu. Vtimellm: Empower llm to grasp
 603 video moments. In *Proceedings of the IEEE/CVF Conference on Computer Vision and Pattern
 604 Recognition*, pp. 14271–14280, 2024.

605

606 OpenAI: Aaron Hurst, Adam Lerer, Adam P. Goucher, Adam Perelman, Aditya Ramesh, Aidan
 607 Clark, AJ Ostrow, Akila Welihinda, Alan Hayes, Alec Radford, Aleksander Mądry, Alex Baker-
 608 Whitcomb, Alex Beutel, Alex Borzunov, Alex Carney, Alex Chow, Alex Kirillov, Alex Nichol,
 609 Alex Paino, Alex Renzin, Alex Tachard Passos, Alexander Kirillov, Alexi Christakis, Alexis Con-
 610 neau, Ali Kamali, Allan Jabri, Allison Moyer, Allison Tam, Amadou Crookes, Amin Tootoochian,
 611 Amin Tootoonchian, Ananya Kumar, Andrea Vallone, Andrej Karpathy, Andrew Braunstein,
 612 Andrew Cann, Andrew Codispoti, Andrew Galu, Andrew Kondrich, Andrew Tulloch, Andrey
 613 Mishchenko, Angela Baek, Angela Jiang, Antoine Pelisse, Antonia Woodford, Anuj Gosalia,
 614 Arka Dhar, Ashley Pantuliano, Avi Nayak, Avital Oliver, Barret Zoph, Behrooz Ghorbani, Ben
 615 Leimberger, Ben Rossen, Ben Sokolowsky, Ben Wang, Benjamin Zweig, Beth Hoover, Blake
 616 Samic, Bob McGrew, Bobby Spero, Bogo Giertler, Bowen Cheng, Brad Lightcap, Brandon
 617 Walkin, Brendan Quinn, Brian Guaraci, Brian Hsu, Bright Kellogg, Brydon Eastman, Camillo
 618 Lugaressi, Carroll Wainwright, Cary Bassin, Cary Hudson, Casey Chu, Chad Nelson, Chak Li,
 619 Chan Jun Shern, Channing Conger, Charlotte Barette, Chelsea Voss, Chen Ding, Cheng Lu,
 620 Chong Zhang, Chris Beaumont, Chris Hallacy, Chris Koch, Christian Gibson, Christina Kim,
 621 Christine Choi, Christine McLeavey, Christopher Hesse, Claudia Fischer, Clemens Winter, Coley
 622 Czarnecki, Colin Jarvis, Colin Wei, Constantin Koumouzelis, Dane Sherburn, Daniel Kappler,
 623 Daniel Levin, Daniel Levy, David Carr, David Farhi, David Mely, David Robinson, David Sasaki,
 624 Denny Jin, Dev Valladares, Dimitris Tsipras, Doug Li, Duc Phong Nguyen, Duncan Findlay,
 625 Edede Oiwoh, Edmund Wong, Ehsan Asdar, Elizabeth Proehl, Elizabeth Yang, Eric Antonow,
 626 Eric Kramer, Eric Peterson, Eric Sigler, Eric Wallace, Eugene Brevdo, Evan Mays, Farzad Kho-
 627 rasani, Felipe Petroski Such, Filippo Raso, Francis Zhang, Fred von Lohmann, Freddie Sulit,
 628 Gabriel Goh, Gene Oden, Geoff Salmon, Giulio Starace, Greg Brockman, Hadi Salman, Haiming
 629 Bao, Haitang Hu, Hannah Wong, Haoyu Wang, Heather Schmidt, Heather Whitney, Heewoo Jun,
 630 Hendrik Kirchner, Henrique Ponde de Oliveira Pinto, Hongyu Ren, Huiwen Chang, Hyung Won
 631 Chung, Ian Kivlichan, Ian O’Connell, Ian O’Connell, Ian Osband, Ian Silber, Ian Sohl, Ibrahim
 632 Okuyucu, Ikkai Lan, Ilya Kostrikov, Ilya Sutskever, Ingmar Kanitscheider, Ishaan Gulrajani,
 633 Jacob Coxon, Jacob Menick, Jakub Pachocki, James Aung, James Betker, James Crooks, James
 634 Lennon, Jamie Kiros, Jan Leike, Jane Park, Jason Kwon, Jason Phang, Jason Teplitz, Jason Wei,
 635 Jason Wolfe, Jay Chen, Jeff Harris, Jenia Varavva, Jessica Gan Lee, Jessica Shieh, Ji Lin, Jiahui
 636 Yu, Jiayi Weng, Jie Tang, Jieqi Yu, Joanne Jang, Joaquin Quinonero Candela, Joe Beutler, Joe
 637 Landers, Joel Parish, Johannes Heidecke, John Schulman, Jonathan Lachman, Jonathan McKay,
 638 Jonathan Uesato, Jonathan Ward, Jong Wook Kim, Joost Huizinga, Jordan Sitkin, Jos Kraaijveld,
 639 Josh Gross, Josh Kaplan, Josh Snyder, Joshua Achiam, Joy Jiao, Joyce Lee, Juntang Zhuang,
 640 Justyn Harriman, Kai Fricke, Kai Hayashi, Karan Singhal, Katy Shi, Kavin Karthik, Kayla Wood,
 641 Kendra Rimbach, Kenny Hsu, Kenny Nguyen, Keren Gu-Lemberg, Kevin Button, Kevin Liu, Kiel
 642 Howe, Krithika Muthukumar, Kyle Luther, Lama Ahmad, Larry Kai, Lauren Itow, Lauren Work-
 643 man, Leher Pathak, Leo Chen, Li Jing, Lia Guy, Liam Fedus, Liang Zhou, Lien Mamitsuka,
 644 Lilian Weng, Lindsay McCallum, Lindsey Held, Long Ouyang, Louis Feuvrier, Lu Zhang, Lukas
 645 Kondraciuk, Lukasz Kaiser, Luke Hewitt, Luke Metz, Lyric Doshi, Mada Aflak, Maddie Simens,
 646 Madelaine Boyd, Madeleine Thompson, Marat Dukhan, Mark Chen, Mark Gray, Mark Hudnall,
 647 Marvin Zhang, Marwan Aljubeh, Mateusz Litwin, Matthew Zeng, Max Johnson, Maya Shetty,
 648 Mayank Gupta, Meghan Shah, Mehmet Yatbaz, Meng Jia Yang, Mengchao Zhong, Mia Glaese,
 649 Mianna Chen, Michael Janner, Michael Lampe, Michael Petrov, Michael Wu, Michele Wang,
 650 Michelle Fradin, Michelle Pokrass, Miguel Castro, Miguel Oom Temudo de Castro, Mikhail
 651 Pavlov, Miles Brundage, Miles Wang, Minal Khan, Mira Murati, Mo Bavarian, Molly Lin, Murat
 652 Yesildal, Nacho Soto, Natalia Gimelshein, Natalie Cone, Natalie Staudacher, Natalie Summers,

648 Natan LaFontaine, Neil Chowdhury, Nick Ryder, Nick Stathas, Nick Turley, Nik Tezak, Niko Fe-
 649 lix, Nithanth Kudige, Nitish Keskar, Noah Deutsch, Noel Bundick, Nora Puckett, Ofir Nachum,
 650 Ola Okelola, Oleg Boiko, Oleg Murk, Oliver Jaffe, Olivia Watkins, Olivier Godement, Owen
 651 Campbell-Moore, Patrick Chao, Paul McMillan, Pavel Belov, Peng Su, Peter Bak, Peter Bakkum,
 652 Peter Deng, Peter Dolan, Peter Hoeschele, Peter Welinder, Phil Tillet, Philip Pronin, Philippe
 653 Tillet, Prafulla Dhariwal, Qiming Yuan, Rachel Dias, Rachel Lim, Rahul Arora, Rajan Troll, Ran-
 654 dall Lin, Rapha Gontijo Lopes, Raul Puri, Reah Miyara, Reimar Leike, Renaud Gaubert, Reza
 655 Zamani, Ricky Wang, Rob Donnelly, Rob Honsby, Rocky Smith, Rohan Sahai, Rohit Ramchan-
 656 dani, Romain Huet, Rory Carmichael, Rowan Zellers, Roy Chen, Ruby Chen, Ruslan Nigmat-
 657 ullin, Ryan Cheu, Saachi Jain, Sam Altman, Sam Schoenholz, Sam Toizer, Samuel Miserendino,
 658 Sandhini Agarwal, Sara Culver, Scott Ethersmith, Scott Gray, Sean Grove, Sean Metzger, Shamez
 659 Hermani, Shantanu Jain, Shengjia Zhao, Sherwin Wu, Shino Jomoto, Shirong Wu, Shuaiqi, Xia,
 660 Sonia Phene, Spencer Papay, Srinivas Narayanan, Steve Coffey, Steve Lee, Stewart Hall, Suchir
 661 Balaji, Tal Broda, Tal Stramer, Tao Xu, Tarun Gogineni, Taya Christianson, Ted Sanders, Tejal
 662 Patwardhan, Thomas Cunningham, Thomas Degry, Thomas Dimson, Thomas Raoux, Thomas
 663 Shadwell, Tianhao Zheng, Todd Underwood, Todor Markov, Toki Sherbakov, Tom Rubin, Tom
 664 Stasi, Tomer Kaftan, Tristan Heywood, Troy Peterson, Tyce Walters, Tyna Eloundou, Valerie Qi,
 665 Veit Moeller, Vinnie Monaco, Vishal Kuo, Vlad Fomenko, Wayne Chang, Weiyi Zheng, Wenda
 666 Zhou, Wesam Manassra, Will Sheu, Wojciech Zaremba, Yash Patil, Yilei Qian, Yongjik Kim,
 667 Youlong Cheng, Yu Zhang, Yuchen He, Yuchen Zhang, Yujia Jin, Yunxing Dai, and Yury Malkov.
 668 Gpt-4o system card, 2024. URL <https://arxiv.org/abs/2410.21276>.

669 Peng Jin, Ryuichi Takanobu, Caiwan Zhang, Xiaochun Cao, and Li Yuan. Chat-univi: Unified vi-
 670 sual representation empowers large language models with image and video understanding. *arXiv*
 671 preprint [arXiv:2311.08046](https://arxiv.org/abs/2311.08046), 2023.

672 Ranjay Krishna, Kenji Hata, Frederic Ren, Li Fei-Fei, and Juan Carlos Niebles. Dense-captioning
 673 events in videos. In *2017 IEEE International Conference on Computer Vision (ICCV)*, pp. 706–
 674 715, 2017. doi: 10.1109/ICCV.2017.83.

675 Bo Li, Yuanhan Zhang, Dong Guo, Renrui Zhang, Feng Li, Hao Zhang, Kaichen Zhang, Yanwei
 676 Li, Ziwei Liu, and Chunyuan Li. Llava-onevision: Easy visual task transfer. *arXiv* preprint
 677 [arXiv:2408.03326](https://arxiv.org/abs/2408.03326), 2024a.

678 KunChang Li, Yinan He, Yi Wang, Yizhuo Li, Wenhai Wang, Ping Luo, Yali Wang, Limin Wang,
 679 and Yu Qiao. Videochat: Chat-centric video understanding. *arXiv* preprint [arXiv:2305.06355](https://arxiv.org/abs/2305.06355),
 680 2023.

681 Yanwei Li, Chengyao Wang, and Jiaya Jia. Llama-vid: An image is worth 2 tokens in large language
 682 models. In *European Conference on Computer Vision*, pp. 323–340. Springer, 2024b.

683 Bin Lin, Bin Zhu, Yang Ye, Munan Ning, Peng Jin, and Li Yuan. Video-llava: Learning united
 684 visual representation by alignment before projection. *arXiv* preprint [arXiv:2311.10122](https://arxiv.org/abs/2311.10122), 2023.

685 Jiajun Liu, Yibing Wang, Hanghang Ma, Xiaoping Wu, Xiaoqi Ma, and Jie Hu. Kangaroo: A
 686 powerful video-language model supporting long-context video input, July 2024a. URL <https://kangaroogroup.github.io/Kangaroo.github.io/>.

687 Ruyang Liu, Chen Li, Haoran Tang, Yixiao Ge, Ying Shan, and Ge Li. St-llm: Large language
 688 models are effective temporal learners. <https://arxiv.org/abs/2404.00308>, 2023.

689 Shuming Liu, Chen Zhao, Tianqi Xu, and Bernard Ghanem. BOLT: Boost Large Vision-Language
 690 Model Without Training for Long-form Video Understanding, a. URL [http://arxiv.org/abs/2503.21483](https://arxiv.org/abs/2503.21483).

691 Ye Liu, Zongyang Ma, Zhongang Qi, Yang Wu, Chang Wen Chen, and Ying Shan. E.t. bench: To-
 692 wards open-ended event-level video-language understanding. In *Neural Information Processing
 693 Systems (NeurIPS)*, 2024b.

694 Zijia Liu, Peixuan Han, Haofei Yu, Haoru Li, and Jiaxuan You. Time-R1: Towards Comprehensive
 695 Temporal Reasoning in LLMs, b. URL [http://arxiv.org/abs/2505.13508](https://arxiv.org/abs/2505.13508).

702 Dezhao Luo, Jiabo Huang, Shaogang Gong, Hailin Jin, and Yang Liu. Towards generalisable video
 703 moment retrieval: Visual-dynamic injection to image-text pre-training. In *Proceedings of the*
 704 *IEEE/CVF Conference on Computer Vision and Pattern Recognition*, pp. 23045–23055, 2023a.
 705

706 Ruipu Luo, Ziwing Zhao, Min Yang, Junwei Dong, Minghui Qiu, Pengcheng Lu, Tao Wang, and
 707 Zhongyu Wei. Valley: Video assistant with large language model enhanced ability, 2023b.
 708

709 Muhammad Maaz, Hanoona Rasheed, Salman Khan, and Fahad Shahbaz Khan. Video-chatgpt:
 710 Towards detailed video understanding via large vision and language models. *arXiv preprint*
 711 *arXiv:2306.05424*, 2023.
 712

713 OpenAI. Gpt-4o mini: Advancing cost-efficient intelligence. <https://openai.com/blog/gpt-4o>, 2024. Accessed: 2025-05-16.
 714

715 OpenGVLab Team. Internvl2: Better than the best—expanding performance boundaries of
 716 open-source multimodal models with the progressive scaling strategy, 2024. URL <https://internvl.github.io/blog/2024-07-02-InternVL-2.0/>. Accessed: 2025-05-16.
 717

718 Long Qian, Juncheng Li, Yu Wu, Yaobo Ye, Hao Fei, Tat-Seng Chua, Yuetong Zhuang, and Siliang
 719 Tang. Momentor: Advancing video large language model with fine-grained temporal reasoning,
 720 2024.
 721

722 Mengxue Qu, Xiaodong Chen, Wu Liu, Alicia Li, and Yao Zhao. ChatVTG: Video Temporal
 723 Grounding via Chat with Video Dialogue Large Language Models . In *2024 IEEE/CVF Conference on Computer Vision and Pattern Recognition Workshops (CVPRW)*, pp. 1847–1856, Los
 724 Alamitos, CA, USA, June 2024. IEEE Computer Society. doi: 10.1109/CVPRW63382.2024.
 725 00191. URL <https://doi.ieee.org/10.1109/CVPRW63382.2024.00191>.
 726

727 Alec Radford, Jong Wook Kim, Chris Hallacy, Aditya Ramesh, Gabriel Goh, Sandhini Agarwal,
 728 Girish Sastry, Amanda Askell, Pamela Mishkin, Jack Clark, et al. Learning transferable visual
 729 models from natural language supervision. In *International conference on machine learning*, pp.
 730 8748–8763. PMLR, 2021.
 731

732 Shuhuai Ren, Linli Yao, Shicheng Li, Xu Sun, and Lu Hou. Timechat: A time-sensitive multimodal
 733 large language model for long video understanding. *ArXiv*, abs/2312.02051, 2023.
 734

735 Xi Tang, Jihao Qiu, Lingxi Xie, Yunjie Tian, Jianbin Jiao, and Qixiang Ye. Adaptive keyframe
 736 sampling for long video understanding. *ArXiv*, abs/2502.21271, 2025. URL <https://api.semanticscholar.org/CorpusID:276725474>.
 737

738 Gemini Team, Petko Georgiev, Ving Ian Lei, Ryan Burnell, Libin Bai, Anmol Gulati, Garrett Tanzer,
 739 Damien Vincent, Zhufeng Pan, Shibo Wang, et al. Gemini 1.5: Unlocking multimodal under-
 740 standing across millions of tokens of context. *arXiv preprint arXiv:2403.05530*, 2024.
 741

742 Qwen Team. Qwen2.5-vl, January 2025. URL <https://qwenlm.github.io/blog/qwen2.5-vl/>.
 743

744 Peng Wang, Shuai Bai, Sinan Tan, Shijie Wang, Zhihao Fan, Jinze Bai, Keqin Chen, Xuejing Liu,
 745 Jialin Wang, Wenbin Ge, Yang Fan, Kai Dang, Mengfei Du, Xuancheng Ren, Rui Men, Dayiheng
 746 Liu, Chang Zhou, Jingren Zhou, and Junyang Lin. Qwen2-vl: Enhancing vision-language model’s
 747 perception of the world at any resolution. *arXiv preprint arXiv:2409.12191*, 2024.
 748

749 Haoning Wu, Dongxu Li, Bei Chen, and Junnan Li. LongVideoBench: A Benchmark for
 750 Long-context Interleaved Video-Language Understanding. URL <http://arxiv.org/abs/2407.15754>.
 751

752 Yuxuan Yan, Shiqi Jiang, Ting Cao, Yifan Yang, Qianqian Yang, Yuanchao Shu, Yuqing Yang,
 753 and Lili Qiu. Empowering agentic video analytics systems with video language models. *arXiv*
 754 *preprint arXiv:2505.00254*, 2025.
 755

756 Ziang Yan, Zhilin Li, Yinan He, Chenting Wang, Kunchang Li, Xinhao Li, Xiangyu Zeng, Zilei
 757 Wang, Yali Wang, Yu Qiao, Limin Wang, and Yi Wang. Task preference optimization: Improving
 758 multimodal large language models with vision task alignment. *arXiv preprint arXiv:2412.19326*,
 759 2024.

760 Yuan Yao, Tianyu Yu, Ao Zhang, Chongyi Wang, Junbo Cui, Hongji Zhu, Tianchi Cai, Haoyu Li,
 761 Weilin Zhao, Zihui He, et al. Minicpm-v: A gpt-4v level mllm on your phone. *arXiv preprint*
 762 *arXiv:2408.01800*, 2024.

764 Hang Zhang, Xin Li, and Lidong Bing. Video-llama: An instruction-tuned audio-visual language
 765 model for video understanding. *arXiv preprint arXiv:2306.02858*, 2023.

766 Peiyuan Zhang, Kaichen Zhang, Bo Li, Guangtao Zeng, Jingkang Yang, Yuanhan Zhang, Ziyue
 767 Wang, Haoran Tan, Chunyuan Li, and Ziwei Liu. Long context transfer from language to vision.
 768 *arXiv preprint arXiv:2406.16852*, 2024a. URL <https://arxiv.org/abs/2406.16852>.

769 Peiyuan Zhang, Kaichen Zhang, Bo Li, Guangtao Zeng, Jingkang Yang, Yuanhan Zhang, Ziyue
 770 Wang, Haoran Tan, Chunyuan Li, and Ziwei Liu. Long context transfer from language to vision.
 771 *arXiv preprint arXiv:2406.16852*, 2024b.

773 Songyang Zhang, Houwen Peng, Jianlong Fu, and Jiebo Luo. Learning 2d temporal adjacent net-
 774 works formoment localization with natural language. In *The IEEE Conference on Computer*
 775 *Vision and Pattern Recognition (AAAI)*, 2020.

776 Yukang Zhang, Yan Yan, Yang Lu, and Hanzi Wang. Towards a unified middle modality learning-
 777 ing for visible-infrared person re-identification. In *Proceedings of the 29th ACM International*
 778 *Conference on Multimedia*, pp. 788–796, 2021.

780 Jianing Zhao, Jingjing Wang, Yujie Jin, Jiamin Luo, and Guodong Zhou. Hawkeye: Discovering and
 781 grounding implicit anomalous sentiment in recon-videos via scene-enhanced video large language
 782 model. In *ACM Multimedia 2024*, 2024. URL <https://openreview.net/forum?id=ys3V4jiENk>.

785 A MORE EVALUATION RESULTS 7B MODELS

787 We further enhance Qwen2.5-VL-7B model with our two-stage RL training pipeline *ViTL* and com-
 788 pare the results on temporal grounding task and QA answering task on Charade-STA (Gao et al.,
 789 2017) and CG-Bench (Chen et al., 2024a).

790 **Charades-STA (Gao et al., 2017).** As presented in Table 10, **ViTL (Ours 7B)** achieves strong per-
 791 formance, outperforming several specialized methods in mIoU and recall at various IoU thresholds.
 792 The **ViTL (Ours 3B)** variant also shows competitive results.

794 Table 10: Zero-shot Video Temporal Grounding on Charades-STA (Gao et al., 2017). **Bold** indicates
 795 our model’s results and its scores.

797 Method	798 Size	799 R@0.3 (%)\uparrow	800 R@0.5 (%)\uparrow	801 R@0.7 (%)\uparrow	802 mIoU (%)\uparrow
VTimeLLM (Huang et al., 2024)	13B	55.3	34.3	14.7	34.6
TimeChat (Ren et al., 2023)	7B	51.5	32.2	13.4	–
Momentor (Qian et al., 2024)	7B	42.6	26.6	11.6	28.5
HawkEye (Zhao et al., 2024)	7B	50.6	31.4	14.5	33.7
ChatVTG (Qu et al., 2024)	7B	52.7	33.0	15.9	34.9
VideoChat-TPO (Yan et al., 2024)	7B	58.3	40.2	18.4	38.1
E.T. Chat (Liu et al., 2024b)	4B	65.7	45.9	20.0	42.3
ViTL (Ours 3B)	3B	77.7	63.5	36.3	54.0
ViTL (Ours 7B)	7B	80.1	66.0	40.2	59.0

808 **CG-Bench (Chen et al., 2024a).** Table 11 shows that **ViTL (Ours 3B)** and **ViTL (Ours 7B)**
 809 achieves competitive mIoU for grounding compared to other models of similar and larger sizes,
 while also providing a strong long-form accuracy.

810
 811 Table 11: Grounded VideoQA performance on CG-Bench. Closed-source APIs (top) and open-
 812 source models (bottom) are grouped separately and sorted by parameter size. **Bold** indicates our
 813 model’s results and its scores. *ViTL* (3B/7B) consistently outperforms open-source baselines of
 814 similar and larger sizes in grounding quality (mIoU).

Method	Size	Type	long-acc. (%)↑	mIoU (%)↑
<i>Closed-source (API)</i>				
Gemini-1.5-Flash (Team et al., 2024)	–	API	32.3	3.67
GPT-4o-mini (OpenAI, 2024)	–	API	33.4	3.75
Gemini-1.5-Pro (Team et al., 2024)	–	API	37.2	3.95
Claude-3.5-Sonnet (Anthropic, 2024)	–	API	40.5	3.99
GPT-4o (OpenAI, 2024)	–	API	45.2	5.62
<i>Open-source models</i>				
Qwen2.5VL-instruct (Team, 2025)	3B	Open	18.4	0.86
ViTL (Ours 3B)	3B	Open	23.5	2.90
Video-LLaVA (Lin et al., 2023)	7B	Open	16.2	1.13
VideoLLaMA 2 (Zhang et al., 2023)	7B	Open	18.4	1.21
Videochat2 (Li et al., 2023)	7B	Open	19.3	1.28
Qwen-VL-Chat (Bai et al., 2023)	7B	Open	21.6	0.89
ST-LLM (Liu et al., 2023)	7B	Open	23.8	2.23
LongVA (Zhang et al., 2024a)	7B	Open	28.7	2.94
LLaVA-OV (Li et al., 2024a)	7B	Open	31.1	1.63
ViTL (Ours 7B)	7B	Open	34.4	3.32
MiniCPM-v2.6 (Yao et al., 2024)	8B	Open	30.1	2.35
Kangaroo (Liu et al., 2024a)	8B	Open	30.2	2.56
Chat-UniVi-v1.5 (Jin et al., 2023)	13B	Open	25.9	2.07
Video-CCAM (Fei et al., 2024)	14B	Open	29.7	2.63
ShareGPT4Video (Chen et al., 2024b)	16B	Open	26.7	1.85
VITA (Fu et al., 2024)	8×7B	Open	33.3	3.06
Qwen2-VL (Wang et al., 2024)	72B	Open	41.3	3.58
InternVL2 (OpenGVLab Team, 2024)	78B	Open	42.2	3.91

B ADDITIONAL ANALYSES AND DISCUSSIONS

B.1 ROBUSTNESS TO TEMPORAL GROUNDING BIAS AND QVHIGHLIGHTS TRANSFER

844 A recent line of work shows that temporal grounding models often exploit dataset-specific priors
 845 (e.g., typical moment location and duration) instead of learning true cross-modal reasoning. To verify
 846 that *ViTL* does not rely on such priors, we evaluate it on ActivityNet-CD, an out-of-distribution
 847 (OOD) split of ActivityNet-Captions specifically constructed to break these biases, and further per-
 848 form zero-shot moment retrieval on QVHighlights.

849 As shown in Table 12, *ViTL* (7B) maintains strong performance under distribution shift: its mIoU
 850 drops only slightly from 24.1 to 23.3 when moving from the in-domain ActivityNet-Captions split to
 851 ActivityNet-CD, while still clearly outperforming the Qwen2.5-VL-7B baseline in both settings. On
 852 QVHighlights zero-shot transfer, *ViTL* also improves mAP@5 by +1.3 absolute (14.2 vs. 12.9), sup-
 853 porting that our “Skim-Zoom” pipeline learns query-conditioned grounding rather than memorizing
 854 temporal priors.

855
 856 Table 12: In-domain vs. distribution-shift generalization and zero-shot transfer. *ViTL* main-
 857 tains strong performance on ActivityNet-CD (OOD) and improves zero-shot moment retrieval on
 858 QVHighlights.

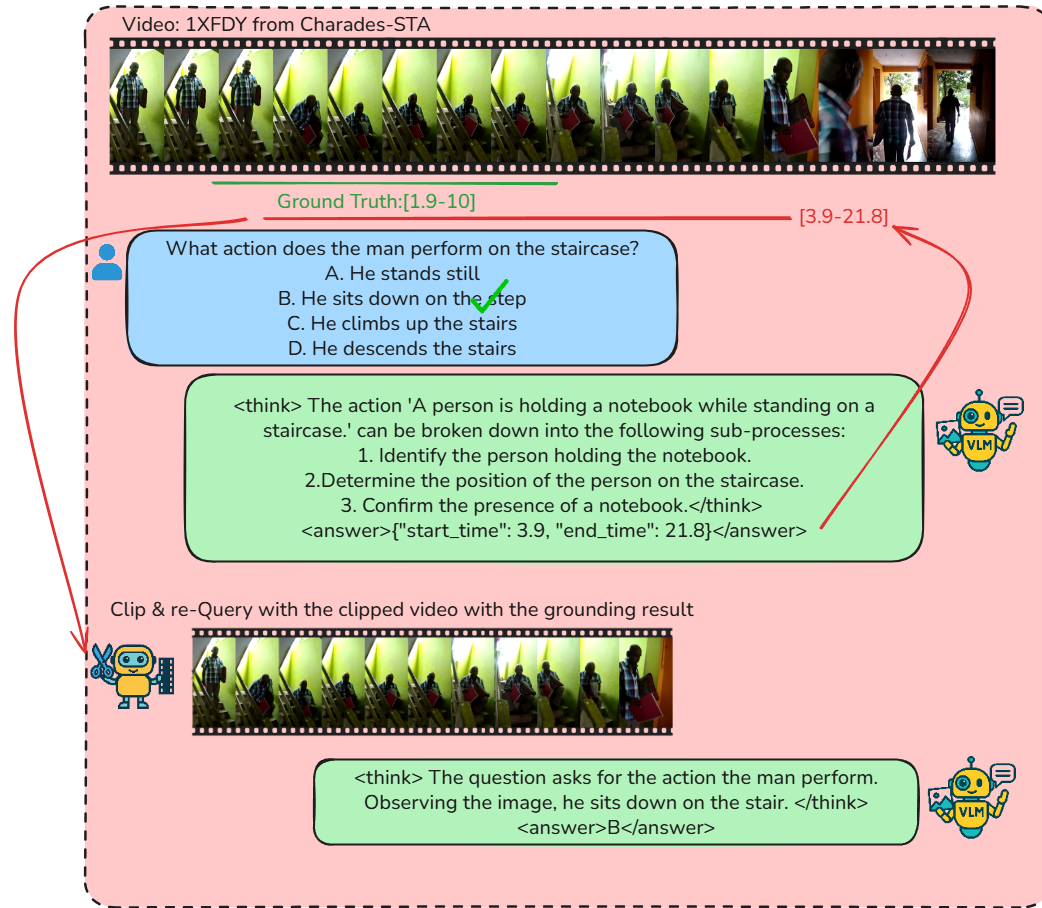
Dataset	Setting	Metric	Qwen2.5-VL-7B	ViTL (7B)
ActivityNet-Captions	In-domain (Train = Test dist.)	mIoU	22.5	24.1
ActivityNet-CD	OOD (distribution-shift)	mIoU	20.2	23.3
QVHighlights	Zero-shot moment retrieval	mAP@5	12.9	14.2

864
865 **B.2 OPEN-ENDED QA CAPABILITIES**866 While our main experiments adopt multiple-choice QA for standardized evaluation, *ViTL* is built on
867 top of generalist MLLMs (Qwen2.5-VL) and naturally supports open-ended generation. To assess
868 these generative capabilities, we evaluate *ViTL* on EgoTempo, an open-ended QA benchmark.869 Table 13 shows that *ViTL* improves open-ended QA accuracy from 26.1% (Qwen2.5-VL-7B) to
870 31.0%, demonstrating that our “Skim–Zoom” temporal grounding also benefits free-form reasoning
871 and not only multiple-choice formats.
872873 Table 13: Open-ended QA performance on EgoTempo. *ViTL* improves open-ended QA accuracy
874 over the Qwen2.5-VL-7B backbone.
875

876 Model	876 Task	876 Accuracy (%)
877 Qwen2.5-VL-7B	877 Open-ended QA	877 26.1
878 <i>ViTL</i> (Ours)	878 Open-ended QA	878 31.0

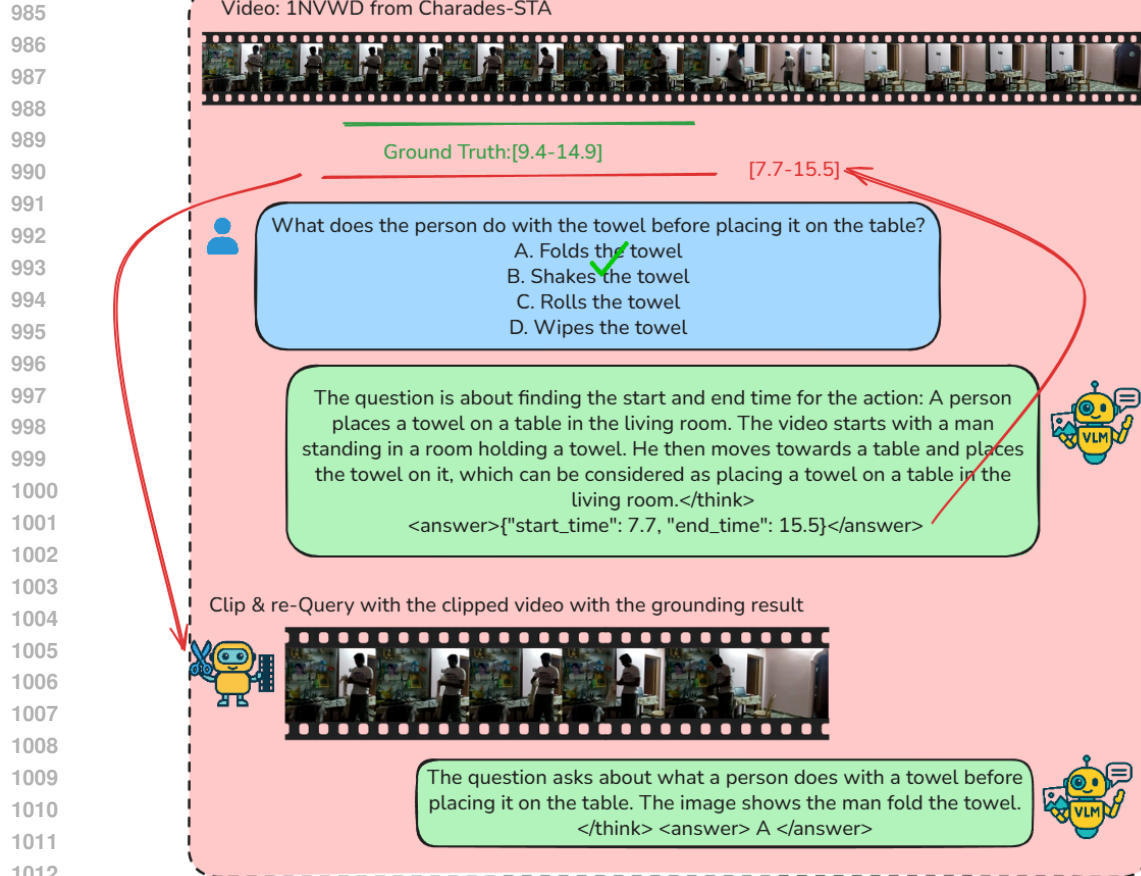
880
881 **C MORE QUALITATIVE RESULTS**
882883 We provide additional qualitative examples of our video-in-the-loop approach in Figure 3, Figure 4,
884 Figure 5 and Figure 6
885886 **D DECLARATION OF LLM USAGE**
887888 We used large language models (LLMs) solely for light editing of prose—including wording refine-
889 ment, grammar correction, and minor clarity improvements—in limited portions of this paper. All
890 LLM-edited text was subsequently reviewed and revised by the authors.
891

918
919
920
921
922
923
924
925
926
927
928
929
930



961 Figure 3: Qualitative demonstration of our two-stage reasoning and grounding pipeline on a sample
962 video from Charade-STA.
963
964
965
966
967
968
969
970
971

972
973
974
975
976
977
978
979
980
981
982
983
984



1013 Figure 4: Qualitative demonstration of our two-stage reasoning and grounding pipeline on a sample
1014 video from Charade-STA.
1015

1016
1017
1018
1019
1020
1021
1022
1023
1024
1025

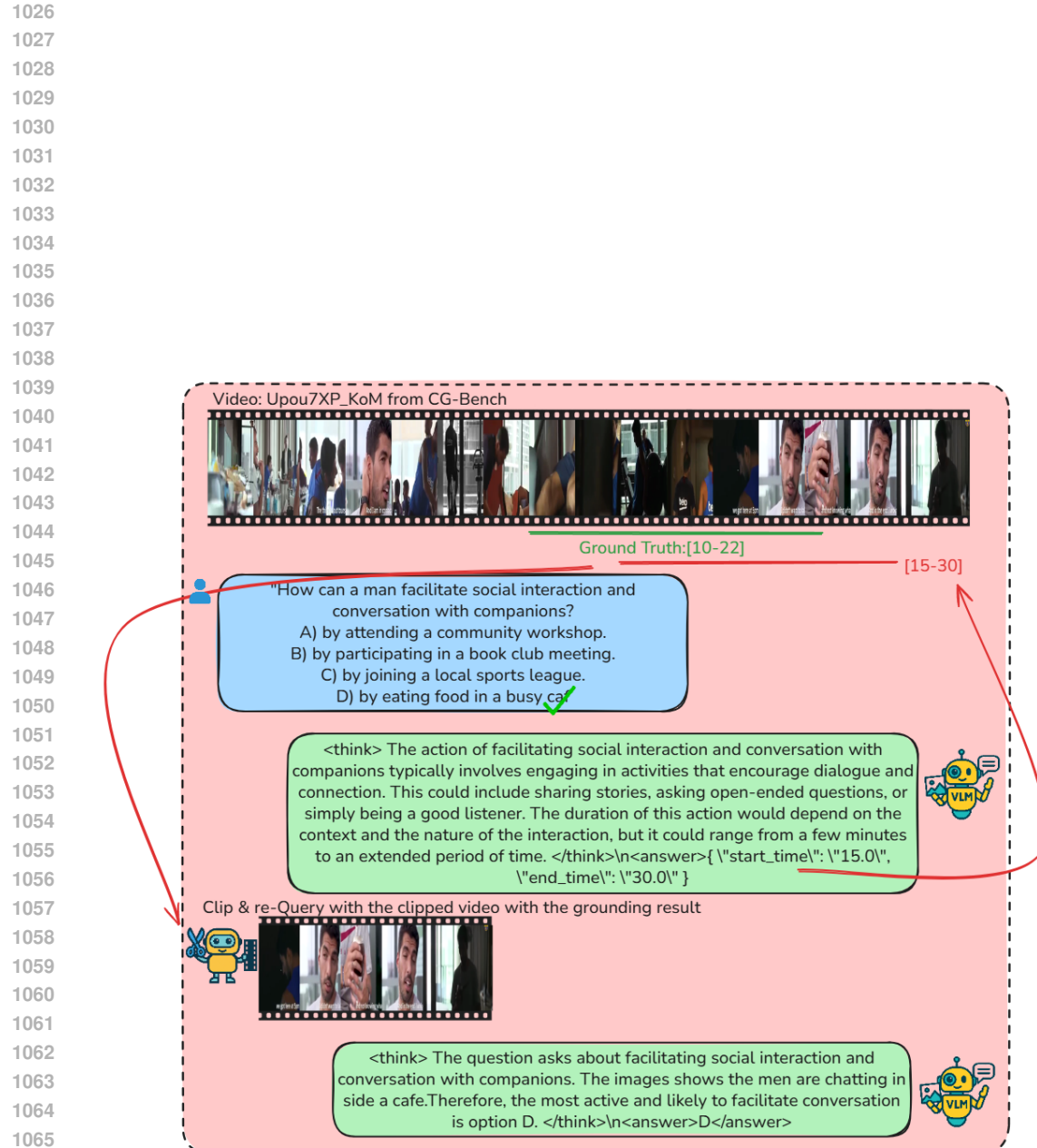


Figure 5: Qualitative demonstration of our two-stage reasoning and grounding pipeline on a sample video from CG-Bench.

